Spatial design and control of graphene flake motion

H. Ghorbanfekr-Kalashami, F. M. Peeters, K. S. Novoselov, and M. Neek-Amal

Spatial design and control of graphene flake motion

H. Ghorbanfekr-Kalashami[1], F. M. Peeters[1], K. S. Novoselov[2], M. Neek-Amal[1]*

[1]Department of Physics, University of Antwerp, Groenenborgerlaan 171, B-2020 Antwerpen, Belgium.

[2]School of Physics and Astronomy, University of Manchester, Manchester M13 9PL, UK.

The force between a sharp scanning probe tip and a surface can drive a graphene flake over crystalline substrates. Recent design of particular patterns of structural defects on a graphene surface allows us to propose an alternative approach for controlling the motion of graphene flake over a graphene substrate. The thermally induced motion of a graphene flake is controlled by engineering topologically defects in the substrate. Such defected regions lead to an inhomogeneous energy landscape and are energetically unfavorable for the motion of the flake, and will invert and scatter graphene flakes when they are moving toward the defected line. Engineering the distribution of these energy barriers results in a controllable trajectory for the thermal motion of the flake without using any external force. We predict superlubricity of the graphene flake for motion along and between particular defect lines. This work provides new insights into frictional forces of interfaces and opens a novel route to the engineering of the stochastic motion of a graphene flake over any crystalline substrate.

I. INTRODUCTION

Atomic scale precision and control of the motion of graphene flakes over crystalline substrates are used for atomic scale design of novel systems targeted for operations at the atomic scale. [1–5] The lateral frictional force between a sharp tip and a surface - for driving a nanometer-sized graphene flakes over the surface of graphite - can be measured by atomic force microscopy (AFM) and scanning tunneling microscopy (STM). [1–3] This is related to the self-reorientation of interacting two-dimensional crystals recently studied for other layered crystals beyond graphene over graphite. [4, 5]

The diffusion after rotation of a graphene flake into superlubric states is controlled by the size of the flake, temperature, and the presence of contamination bubbles or defects in the underlying substrate. For instance, superlubric to commensurate ground states gives longer sliding distance (95 nm) at low temperature 5 K as compared to (33 nm) 77 K. [1] It has also been reported that a misaligned graphene flake (3° rotated) can be returned to the commensurate state by annealing the sample up to 200°C. [4]

On the other hand, recent control over the location and average complexity of defect formation in graphene (by exposure of a graphene sample to a focused electron beam) allowed to engineer defect patterns in a desirable way. [6] Defects in graphene modify its properties and affects its functionality. [7, 8] We are interested to use such designed defects in the substrate to engineer the dynamics of a graphene flake that is put on top of it.

In this letter, we reveal that the superlubricity of a graphene flake over a graphite substrate [9–11] is strongly influenced by the presence of defects in the substrate. The dynamics of the graphene flake is significantly altered and the well known random rotational motion and corresponding transition from incommensurate to commensurate states and related life time are profoundly influenced by the defected regions. In particular, we ob-
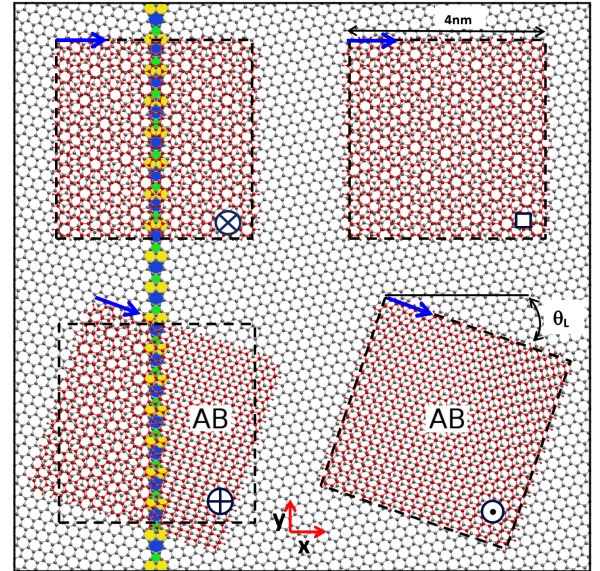

FIG. 1. (color online) A hydrogen edge-passivated flake is put over graphene which initially is in one of the positions labeled by square, $\odot$, $\oplus$, and $\otimes$. The black dashed lines indicate the region that is scanned for finding the energy landscape, see Fig. 2. The blue vector ($\hat{u}_{ac}$) is a unit vector along the armchair direction of the flake which helps us to determine the mutual orientation between the flake and the x-axis of the substrate.

serve backscattering in the motion of a flake that is moved towards a grain boundary (GB) line. Notice that the commensurate to incommensurate transition is the main reason for locking of the flakes on the substrate. This transition is determined by the competition between the GB line size, initial velocity and size of the flake. Several types of grain boundaries - different arrays of 5-7 defects - are investigated in order to identify how they influence the trajectory of motion of a graphene flake. Our work reveal several microscopic aspects of the motion of a thermally actuated flake over graphene with GB which can

be helpful for developing AFM/STM driven force measurements. [1, 2] Although AFM measurements give an estimation for the static friction force, but providing any details on the complex dynamics of the sliding motion of graphene flakes is still challenging [12].

II. THE MODEL AND METHOD

Molecular dynamics simulations are used to simulate a graphene flake with 750 carbon atoms and 72 hydrogen atoms at its edges. The substrate is a graphene layer which contains a GB line at the middle. We study several types of GB where the mutual orientations of the two crystalline domains is described by the misorientation angle which e.g. for Large-Angle Grain Boundary (LAGBI) [7] is $\theta_L =21.8^o$ with respect to x-axis, see Fig. S1 in Supplemental Material (SM) [13] for more grain boundaries. A square-shaped flake (dimension $l^2 = 4\,nm \times 4\,nm$ terminated by hydrogen atoms) is put over the substrate. Such a small size graphene nanoribbon can be fabricated using e.g. bottom-up approach. [14] We associate a unit vector that is always along its armchair direction (independent of its orientation with the substrate $\hat{u}_{ac}$). Therefore the orientation of the flake with respect to the substrate is determined by the angle θ which is defined by $\hat{x}.\hat{u}_{ac} = cos(\theta)$. To model the covalent bonds formed between the different carbon atoms within the same flake, we used the AIREBO potential [15] and a registry-dependent potential developed by Kolmogorov and Crespi (KC [16]) for the interlayer interaction [17] which are implemented in the Large-scale Atomic Molecular Massively Parallel Simulator package LAMMPS [18].

III. ENERGY ANALYSIS: PRISTINE AND LAGBI SYSTEM

In Fig. 1 we depict a graphene substrate containing a LAGBI line which is located at $x=0$ and elongated along the y-axis with a flake put on top of it. A typical incommensurate state for the flake (having $\theta = 0^o$) is shown by the square symbol. The other possible configurations can be as those shown by symbols $\odot, \oplus$, and $\otimes$ which have $\theta = \theta_L$, θ_L, and 0°, respectively (see below). Notice that in the RHS (LHS) of the LAGBI line, the system shown by $\odot$ ($\oplus$) is completely (partially) in the AB-stacking configuration.

First, we relaxed the substrate in the xy-plane, then we made it rigid and studied the dynamics of the top flake. In Fig. 2 we depict three vdW-energy landscapes (2D-density plots) where in all cases the flake (which is located at average height $z=0.34\,nm$ above the substrate) is moved to scan a $4 \times 4\,nm^2$ area (the dashed squares in Fig. 1). The corresponding energy landscape (for scan area indicated by the black dashed square $\odot$ in Fig. 1) is shown in Fig. 2(a). The substrate below

the square $\odot$ consists of pristine graphene (the flake is initially in the AB-stacking configuration). In Fig. 2(b) we show the corresponding profiles along the indicated vertical and horizontal dashed lines. These results are in good agreement with previously reported vdW-energy landscape for graphene over graphite. [10] The energy barriers are found to be about $10\,meV/atom$ which is the energy difference between two well known stacking states in graphite $\Delta_0 = E_{AA} - E_{AB}$ (we set E_{AB} to be the energy reference).

In Figs. 2(c,d) we show the energy landscape and corresponding profiles, respectively, for an energy scan inside the dashed square $\oplus$, i.e. a rotated square with respect to the underlying flake. The blue (dashed red) line in Fig. 2(d) refers to the energy profile along x-axis at $y=0$ (y-axis at $x=0$, i.e. along the GB line). The periodic function for the profile along y-axis (GB line) is as expected - maximum barrier is found to be about $\Delta = 5\,meV/atom$ - however the energy profile along x-axis is unexpected. It is seen that until almost $x \simeq -l/2$ the fluctuations in the solid blue line are negligible (as compared to the dashed red line) and after $x \simeq -l/2$ it oscillates (Δ grows) with nonuniform larger amplitude. The latter is due to the fact that crossing the GB brings us to the AB-stacking region as seen from the right hand side part of the flake $\oplus$ in Fig. 1. The maximum energy barrier is found to be around $10\,meV/atom$ where x varies in the range 1-2 nm. Notice that the flake $\oplus$ is rotated by an angle θ_L with respect to the x-axis. In fact, the flake is affected by very small energy barriers for $x \leq -l/2$, i.e. the superlubricity states. The honeycomb pattern in the right hand side of Fig. 2(c) clearly indicates this effect.

In Fig. 2(e) we plot the energy landscape for a scan of the flake $\otimes$ inside the corresponding black-dashed square shown in Fig. 2. Here the flake in both sides of the GB is located at incommensurate states. The corresponding energy profiles along x- and y-axis are shown in Fig. 2(f). One naturally expects to find periodic oscillations for the energy barriers along the GB line where the maximum barrier is about $0.2\,meV/atom$. However, along the x-axis, only when the flake is close to the GB line (its neighborhood), it is influenced by larger energy barriers of $\sim 0.13\,meV/atom$ ($|x| \leq l/2$). Therefore, although in Fig. 2(f) the energy barriers along x-axis where $|x| \leq l/2$, are larger than both the energy in $|x| \geq l/2$, but they are still much smaller than the energy barrier Δ_0 see also Fig. S2 in SM [13] for the energy barriers against rotation above pristine graphene/LAGBI). Notice that the total barrier energy is $750 \times E$ which is the relevant energy for practical applications. E indicates the calculated energy of the flake per atom. Crudely thinking about the latter energy barriers represented in Fig. 2(d,f) – in comparison to the energy barriers in Figs. 2(a,b) – leads us to conclude that the flake should be able to pass the GB easily at any finite temperature. However, surprisingly, this turns out not to be the case (see backscattering).
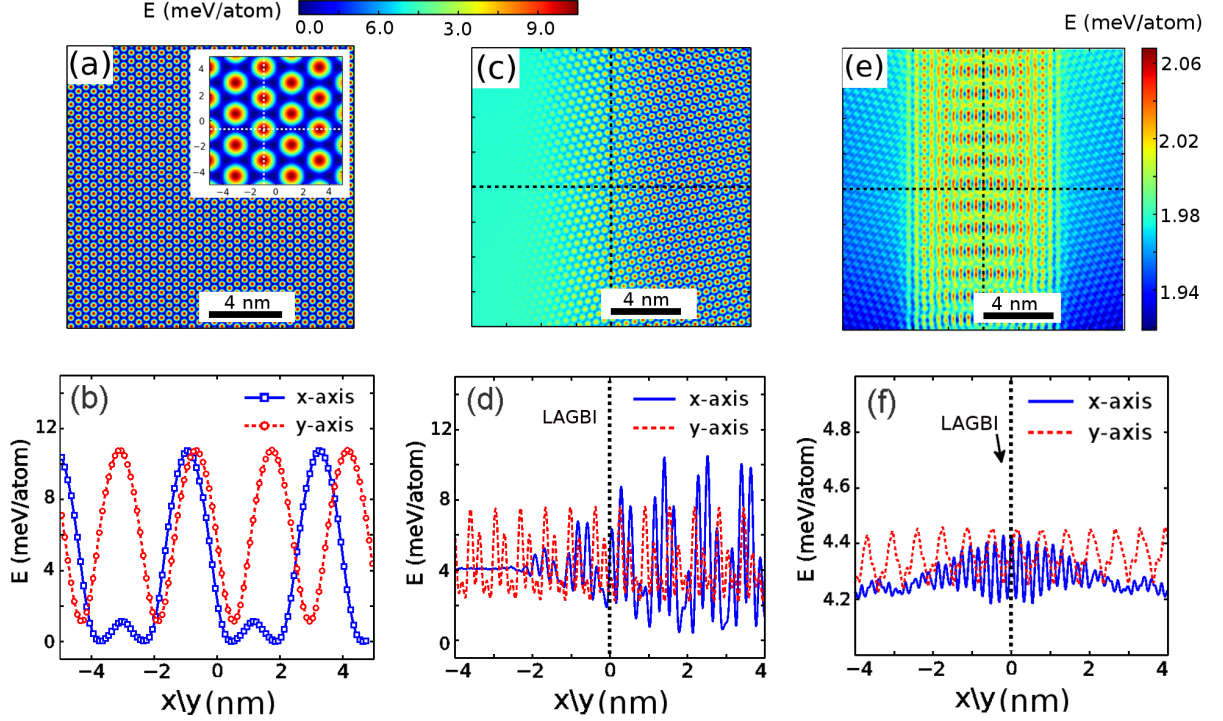
FIG. 2. (color online) (a) The vdW-energy landscape resulting from the vdW-energy stored between the graphene flake above a perfect graphene substrate at z=0.34 nm and (b) two corresponding cross sections along the armchair and zig-zag directions indicated by dashed lines in the inset of (a). In (c) ((e)), we show the energy landscape of the flake rotated with $\theta = \theta_L(0^o)$ scanned inside the box $\oplus$ ($\otimes$) as shown in Fig. 1 and the corresponding cross sections along the dashed lines are shown in (d) ((f)). Energy reference is chosen to be $E_{AB}=0$.
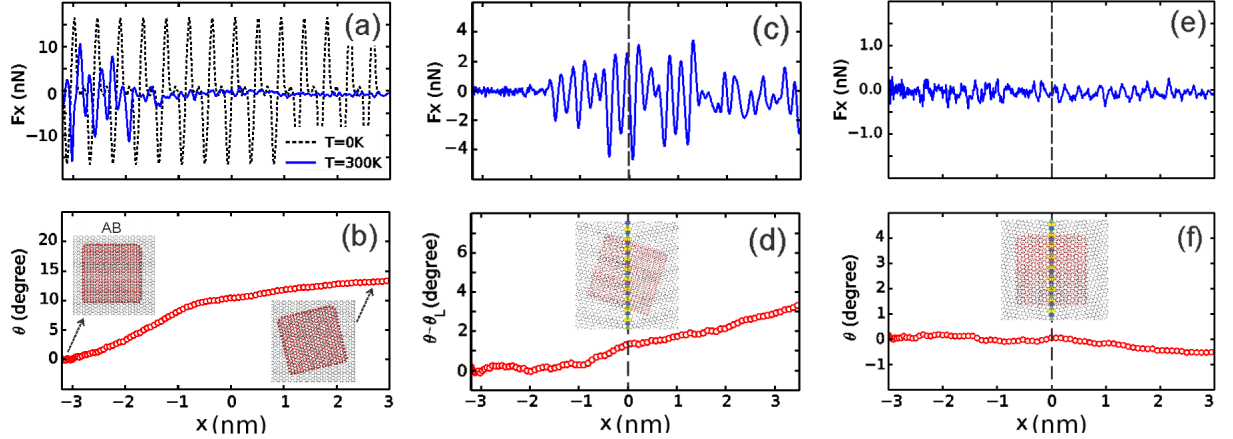

FIG. 3. (color online) The variation of x-component of the total force of a flake moving on (a) pristine graphene, (c,e) a graphene substrate containing a GB line. The variation of corresponding direction θ of the flake are shown in (b,f) and $\theta - \theta_L$ in (d). The orientation of the flake are shown as insets which have 0°, θ_L, and 0° in (b), (d), and (f), respectively.

IV. FORCE ANALYSIS AT FINITE TEMPERATURE

By identifying the force between a sharp tip and a surface, while keeping the temperature fixed at T=300 K [1, 2], frictional effects can be understood. We found that

the lowest force which enables us to move the flake continuously over the GB depends strongly on the initial θ (stacking) of the flake. We applied a constant force of f_0=6.5 pN/atom [20] along the armchair direction which drives the flake (initially started its motion from AB-stacking) to the right. Interestingly, after a shift of about 1 nm (see Fig. 3(a)) the flake rotates (see the variation
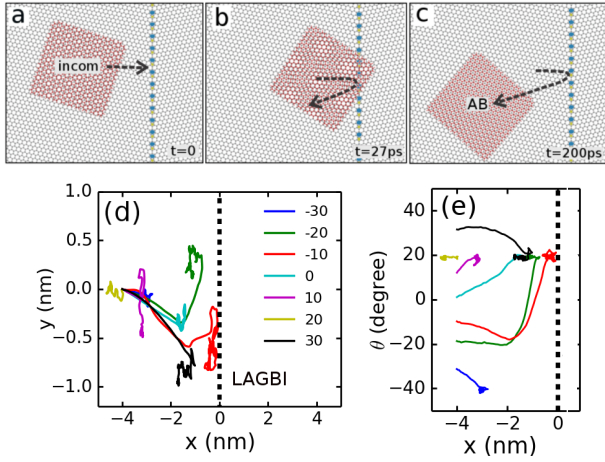
FIG. 4. (color online) Backscattering of a flake moving towards a LAGBI GB when initially it was in an incommensurate state (a,b,c). The path of motion are shown in (d,e) for $v_0 = 100 \, \text{m/s}$ where different colors refer to different initial θ (given in the inset of (d)).

FIG. 5. (color online) (a) The passing probability of a flake with size $4 \, \text{nm} \times 4 \, \text{nm}$ moving over a perfect graphene substrate and three different defected substrates as function of the initial shooting velocity (v_0). In (b), the passing probability for different sizes 3, 4, and 5 nm over LAGBI is shown.

of θ in Fig. 3(b)). In Fig. 3(a) we show the net friction force F_x. The flake rotates and reorients itself after $x \approx -1.5 \, \text{nm}$ in order to minimize its energy.

The dashed line in Fig. 3(a) is the result of sliding the flake over graphene without relaxing it at each step, i.e. a rigid flake is moved with fixed θ along the armchair direction of pristine graphene. Comparing the dashed black line and the blue line leads us to conclude that the results of Ref. [22] are questionable because of the non-relaxed sample.

We also applied f_0 on the flake along the x-axis to move it over the GB line. The results for two different initial θ, i.e. flake $\bigoplus$ with initial $\theta = \theta_L$ and $\bigotimes$ with $\theta = 0^o$, are shown in Figs. 3(c) and 3(e). The corresponding variation of θ is shown in Figs. 3(d) and 3(f), respectively. The flake $\bigoplus$ passes the GB line by experiencing large forces around/on the GB line (Fig. 3(c)) but in parallel it is rotated to minimize its energy. The $\theta - \theta_L$ (see Fig. 3(d)) changes to larger values. The inhomogeneous energy landscape around the GB line creates a lateral force (F_y) on the front of the flake (located in x<-l/2) which induces a net torque ($\tau_z \sim lF_y/2$) and eventually changes the path (note in the beginning $F_y = 0$). The angular velocity can be approximated by $\omega \simeq \sqrt{6(v^2 - v_0^2)/l^2}$ if the initial and current states are incommensurate with small potential energy (e.g. $\omega \simeq 0.01 \, \text{rad/ps}$ for $v_0 = 2v = 100 m/s$).

Surprisingly, when the flake $\bigotimes$ is subjected to f_0, it passes the GB line i.e. $\theta \sim 0^o$ without changing its orientation and it experiences a larger force. In fact if the flake approaches the GB line and is located in the state $\bigotimes$ it can pass the GB line easily, however, this rarely happens because reaching the state $\bigotimes$ is difficult (it is an incommensurate state) except when moving with high kinetic energy. The latter effect is directly related to the
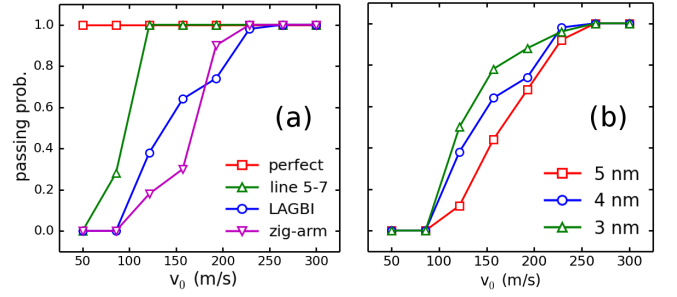
well known superlubricity effect -see Fig. S3 in SM [13] for more detail on the effect of the flake size.

V. BACKSCATTERING

The interface between two domains of graphene with different crystallographic orientation (GB) changes the energy landscape at both sides. If the flake is diffusing on one side of the GB it prefers to stay away from the GB line. In order to quantify this effect, we shoot the graphene flake to the right with initial velocity $\vec{v}_0 = v_0 \hat{x}$ over perfect graphene and given graphene with a GB line where v_0 is the velocity of the center of mass of the flake. The velocity $\vec{v} = (v_x, v_y)$ varies with time after shooting.

In Figs. 4(a-c) we show three different snapshots of a flake moving towards a LAGBI line where initially it started from an incommensurate state. It is clearly seen that the flake is backscattered in (c) when it approaches the GB line. In Fig. 4(d) we show backscattering of the flake moving toward the GB line with different initial θs -see Fig. S4 in SM [13] for a case of moving flake on perfect graphene. The corresponding variation of θ with x are shown in Fig. 4(e) (and velocities are shown in Fig. S5 in SM [13]). Different colors refer to different initial θ which are shown in the legend. The dotted line in Figs. 4(d,e) refers to the LAGBI line. Eventually they arrive into the AB-stacking configuration ("AB" symbol in (c)). [23] Examples of the motion of one such flake are shown in Figs. 4 (a,b,c).

The above described mechanism can be used to design ultra-low dissipation nano mechanical devices. The flake avoids the region over the LAGBI line except for the situation when there are two LAGBI lines on both sides of the flake (panel (b) of Fig. S6 in SM [13]).

VI. DISCUSSION AND CONCLUSIONS

In order to see the influence of the shooting velocity (v_0) of the flake, we show in Fig. 5 the passing probability

as a function of v_0 for perfect and defected substrates (see [25]). By increasing v_0 the passing probability increases. In fact, the lattice orientation on both sides of the GB line determines the passing probability. The smallest passing probability is found for LAGBI (and larger flake with 5 nm size, see Fig. 5(b)) and trivially the largest probability should be for motion over perfect graphene. It is interesting to note that after $x = x_m \simeq -l/2$ most of the flakes start to change their direction of motion (see Fig. 4(d)). Therefore, the flake's portion that enters in the x_m region is affected by LAGBI. [26] We emphasize that the obtained results are general and independent of the shape of the flake, i.e. the minimum energy configuration corresponds to maximizing the commensurate coverage of the flake and substrate independent of its shape.

The design of defect patterns is an active area of research [6, 27], *e.g.* A. W. Robertson *et al.* conducted an experimental study to induce topological atomic defects in graphene using the technique of ion irradiation [6]. Achieving high velocities of the order of 100 m/s for the motion of a flake over a substrate is experimentally challenging. In the past decade, several studies attempted to produce high velocities [28, 29], *e.g.* Nikhil *et al.* use dmodified an existing commercial AFM setup and achieved velocities between $1\,\mu$m/s and $10\,$mm/s [28]. When the flakes move with high supported velocities above the defected regions, we found that the motion can be controlled/scattered by designing particular defect patterns. Our study would be an endeavor worth taking and is promising for the future studies.

The obtained scattering/backscattering (mirror reflection) phenomena can be realized experimentally. Many experimental samples contain GBs and by moving a graphene flake through/over the GB region the motion of the flake should be strongly affected by the presence of the defected region especially when both sides of that region correspond to different crystallographic orientations. For instance, we found that for LAGBI and "zig-arm" substrates see Fig. S1 in SM [13], passing a graphene flake over this GB line has a very small probability, i.e. it only happens for very large v_0 of the flake (see Fig. 6). Moreover, by designing a particular pattern of topological defects on the graphene substrate (see Figs. S6 in SM [13]), thermally induced motion of graphene flakes follows the designed path if the flake can not find an AB-stacking configuration in nearby regions. This is similar to what happens when a flake approaches the edge of the graphene substrate. Such controllable paths can be realized by designing a particular defect pattern on various substrates enabling control of stochastic motion of the flake.

[1] X. Feng, S. Kwon, J. Y. Park, and M. Salmeron, ACS Nano **7**, 1718 (2013).

[2] A. E. Filippov, M. Dienwiebel, J. W. M. Frenken, J. Klafter, and M. Urbakh, Phys. Rev. Lett. **100**, 046102 (2008).

[3] C. M. Mate, G. M. McClelland, R. Erlandsson, and S. Chiang, Phys. Rev. Lett. **159**, 226 (1987).

[4] C. R. Woods, F. Withers, MJ. Zhu, Y. Cao, G. Yu, A. Kozikov, M. Ben. Shalom, S. V. Morozov, M. M. Van Wijk, A. Fasolino, and *et al.* Nat. Comm. **7**, 10800 (2016).

[5] D. Wang, G. Chen, C. Li, M. Cheng, W. Yang, S. Wu, G. Xie, J. Zhang, J. Zhao, X. Lu, and *et al.* Phys. Rev. Lett. **116**, 126101 (2016).

[6] A. W. Robertson, C. S. Allen, Y. A. Wu, K. He, J. Olivier, J. Neethling, A. I. Kirkland, and J. H. Warner, Nat. Comm. **3**, 1144 (2012).

[7] O. V. Yazyev and S. G. Louie, Nat. Mater. **9**, 806 (2010).

[8] D. W. Boukhvalov and M. I. Katsnelson Nano Lett. **8** 4373 (2008).

[9] M. Dienwiebel, G. S. Verhoeven, N. Pradeep, J. W. M. Frenken, J. A. Heimberg, and H. W. Zandbergen, Phys. Rev. Lett. **92**, 126101 (2004).

[10] M. Reguzzoni, A. Fasolino, E. Molinari, and M. C. Righi, Phys. Rev. B **86**, 245434 (2012).

[11] I. V. Lebedeva, A. A. Knizhnik, A. M. Popov, O. V. Ershova, Y. E. Lozovik, and B. V. Potapkin, Phys. Rev. B **82**, 155460 (2010).

[12] S. Kawai, A. Benassi, E. Gnecco, H. Söde, R. Pawlak, X. Feng, K. Müllen, D. Passerone, C.A. Pignedoli, P. Ruffieux, and R. Fasel, Science **351**, 957 (2016).

[13] See Supplemental Material at URL for details of the different defects in the substrate, energy barriers for rotation of flake due to grain boundary LAGBI, variation of the force with size of flake, trajectory above perfect graphene, velocity variations, and channel design.

[14] J. Cai, P. Ruffieux, R. Jaafar, M. Bieri, T. Braun, S. Blankenburg, M. Muoth, A. P. Seitsonen, M. Saleh, X. Feng, K. Müllen, and R. Fasel, Nature **466**, 470 (2010).

[15] S. J. Stuart, A. B. Tutein, and J. A. Harrison, J. Phys. Chem. A **112**, 6472 (2000).

[16] A. N. Kolmogorov and V. H. Crespi, Phys. Rev. B **71**, 235415 (2005).

[17] The AIREBO+KC results in almost the same energy barriers as DFT-D between the flake and the substrate [10]. Notice that a Lennard-Jones (LJ) potential underestimates the experimental and DFT-D energy barrier by an order of magnitude [11] (for more details see Ref. [19])

[18] S. Plimpton, J. Comput. Phys. **117**, 1 (1995).

[19] F. Peymanirad, S. Singh Kumar, H. Ghorbanfekr-Kalashami, K. S. Novoselov, F. M. Peeters, and M. Neek-Amal, 2D Mater. **4**, 025015 (2017).

[20] This force can be approximated by $f_0 \simeq \Delta_0/a_{CC}$ where $a_{CC} = \sqrt{3} \times 1.42$Å. This force might be scaled depending on particle orientation and crystallinity. [21]

[21] D. Dietzel, M. Feldmann, U. D. Schwarz, H. Fuchs, and A. Schirmeisen, Phys. Rev. Lett. **111**, 235502 (2013).

[22] E. Koren and U. Duerig, Phys. Rev. B **94**, 045401 (2016).

[23] Notice that there is a critical length beyond which the super low frictional regime for motion of the flake disappears [24].

[24] M. Ma, A. Benassi, A. Vanossi, and M. Urbakh, Phys. Rev. Lett. **114**, 055501 (2015).

[25] The passing probability in each case was calculated employing an ensemble of different initial incommensurate states. The passing probability for small/large flake can be given by $P_l(v) = 1 - (\frac{v - v_{max}}{\bar{v}})^2$ and $\frac{1}{4}(\frac{v}{v_i} - 1)^2$, respectively shown by triangular and square symbols in Fig. 5(b), where $v_{max} = 3v_i = 3/2\bar{v}$ with v_i=100m/s.

[26] We performed additional simulations for two flakes with different sizes of 3 and 5 nm. We found that the effect of the GB is enhanced when the flake is made larger. Size effects for backscattering demands a new scaling which is different from the one for structural lubricity [21].

[27] J. Lahiri, Y. Lin, P. Bozkurt, I. I. Oleynik, and M. Batzill, Nat. Nanotechnol. **5**, 326 (2010).

[28] N. S. Tambe and B. Bhushan, Nanotechnology **16**, 2309 (2005).

[29] J. Yang, Z. Liu, F. Grey, Z. Xu, X. Li, Y. Liu, M. Urbakh, Y. Cheng, and Q. Zheng, Phys. Rev. Lett. **111**, 029902 (2013).